Please cite this article in press as: Lee et al., An Unconventional Glutamatergic Circuit in the Retina Formed by vGluT3 Amacrine Cells, Neuron (2014), http://dx.doi.org/10.1016/j.neuron.2014.10.021

Neuron
Report

An Unconventional Glutamatergic Circuit in the Retina Formed by vGluT3 Amacrine Cells

Seunghoon Lee,[1,6] Lujing Chen,[1,4,6] Minggang Chen,[1,6] Meijun Ye,[1] Rebecca P. Seal,[5] and Z. Jimmy Zhou[1,2,3,*]
[1]Department of Ophthalmology and Visual Science
[2]Department of Cellular and Molecular Physiology
[3]Department of Neurobiology
Yale University School of Medicine, New Haven, CT 06510, USA
[4]Zhiyuan College, Shanghai Jiao Tong University, Shanghai 200240, China
[5]Department of Neurobiology, University of Pittsburgh School of Medicine, Pittsburgh, PA 15213, USA
[6]Co-first author
*Correspondence: jimmy.zhou@yale.edu
http://dx.doi.org/10.1016/j.neuron.2014.10.021

SUMMARY

In the vertebrate retina, glutamate is traditionally thought to be released only by photoreceptors and bipolar cells to transmit visual signals radially along parallel ON and OFF channels. Lateral interactions in the inner retina are mediated by amacrine cells, which are thought to be inhibitory neurons. Here, we report calcium-dependent glutamate release from vGluT3-expressing amacrine cells (GACs) in the mouse retina. GACs provide an excitatory glutamatergic input to ON-OFF and ON direction-selective ganglion cells and a subpopulation of W3 ganglion cells, but not to starburst amacrine cells. GACs receive excitatory inputs from both ON and OFF channels, generate ON-OFF light responses with a medium-center, wide-surround receptive field structure, and directly regulate ganglion cell activity. The results reveal a functional glutamatergic circuit that mediates noncanonical excitatory interactions in the retina and probably plays a role in generating ON-OFF responses, crossover excitation, and lateral excitation.

INTRODUCTION

Glutamate is known to be released in the retina by photoreceptors (PRs) and bipolar cells (BCs) at ribbon synapses in the outer and inner plexiform layers (OPLs and IPLs), respectively, to mediate radial (vertical) signal processing along ON and OFF visual pathways. Amacrine cells (ACs), which mediate lateral interactions between the vertical visual channels, release either GABA or glycine (Masland, 2012; Wässle et al., 2009). The recent discovery of vesicular glutamate transporter 3 (vGluT3) in a subpopulation of ACs in rat, mouse, and macaque monkey retinae (Fremeau et al., 2002; Gong et al., 2006; Grimes et al., 2011; Haverkamp and Wässle, 2004; Johnson et al., 2004; Stella et al., 2008) raises an intriguing possibility that glutamate may also be released by an AC subtype at conventional (nonribbon) synapses to mediate excitatory interactions in an unconventional way.

GACs comprise a small subset (~1%) of ACs in the mammalian retina. They exhibit immunoreactivity for vGluT3 and glutamate, as well as glycine and glycine transporter GlyT1 (but not vesicular inhibitory amino acid transporter) (Haverkamp and Wässle, 2004; Johnson et al., 2004). They have a medium dendritic field and ramify diffusely between the ON and OFF cholinergic bands (Grimes et al., 2011; Haverkamp and Wässle, 2004; Johnson et al., 2004), allowing them to interact potentially with both the ON and OFF channels. The possibility that GACs receive and release glutamate in both ON and OFF sublaminae of the IPL is fascinating, because it suggests an additional excitatory circuit that is capable of combining ON and OFF excitation and/or mediating lateral excitation between the ON and OFF channels. However, it is unknown whether GACs actually release glutamate as a transmitter, since vGluT3 is also thought to play a role in creating an intracellular store to buffer cytoplasmic glutamate or to facilitate the vesicular transport of another transmitter (El Mestikawy et al., 2011; Johnson et al., 2004). It is also unclear whether GACs receive excitatory inputs from both ON and OFF BCs (Grimes et al., 2011). In order to gain an insight into the physiological role and synaptic circuitry of the vGluT3 system in the retina, several basic questions must be answered. (1) Do GACs actually release glutamate and use it as a classic neurotransmitter? (2) What are the postsynaptic targets of GACs? (3) What are the response polarity and receptive field properties of GACs? (4) What are the functional effects of GACs on their postsynaptic targets?

The present study addressed the above questions using a combination of optogenetics, single and dual patch-clamp recordings, visual stimulation, and two-photon imaging in transgenic mice that had Cre-dependent expression of channel rhodopsin 2 (ChR2) in GACs. We report the functional release of glutamate by GACs, as well as the receptive field properties, postsynaptic targets, and potential postsynaptic actions of GACs.

RESULTS

GACs Provide Excitatory Inputs to Specific Postsynaptic Cell Types

To determine whether GACs make excitatory synapses onto specific postsynaptic neurons, we optically activated

Please cite this article in press as: Lee et al., An Unconventional Glutamatergic Circuit in the Retina Formed by vGluT3 Amacrine Cells, Neuron (2014), http://dx.doi.org/10.1016/j.neuron.2014.10.021

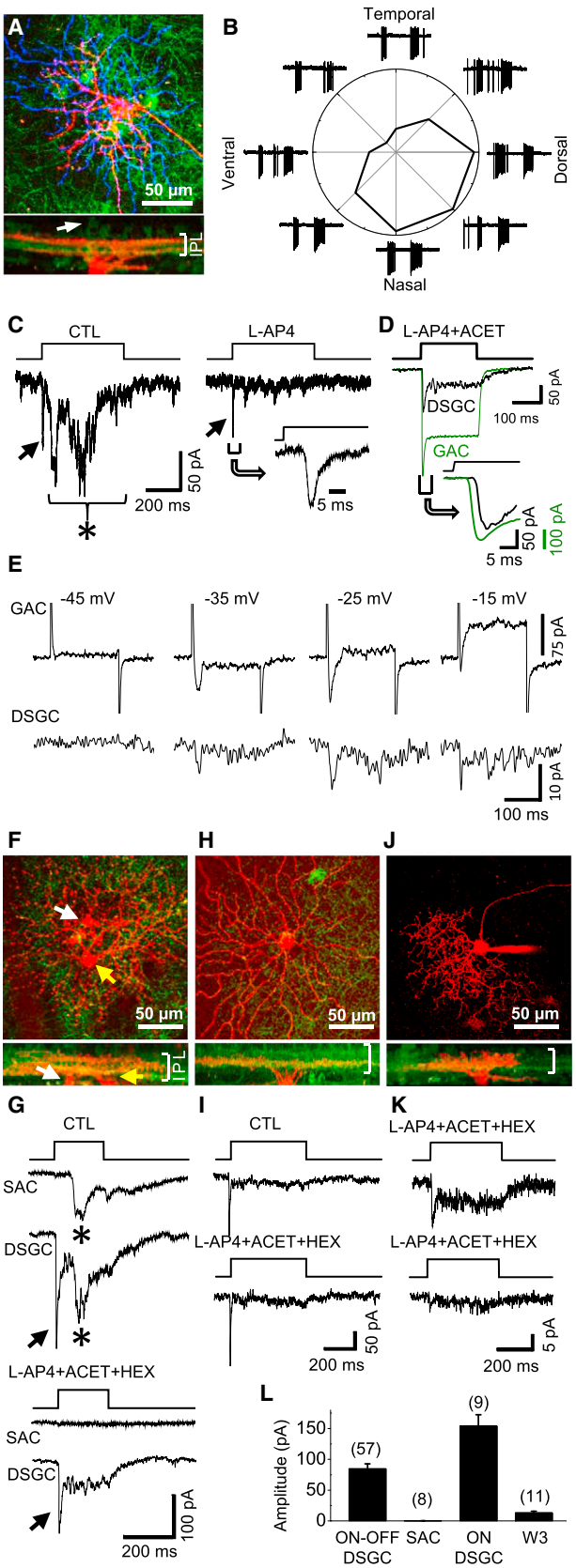

Figure 1. Excitatory Synaptic Transmission from GACs to Specific Postsynaptic Targets

(A) Top: collapsed two-photon images of ON (red) and OFF (blue) dendrites of an ON-OFF DSGC after whole-cell recording in a vGluT3-Cre/ChR2-YFP (green) retina. Bottom: z projection image of the same cell. Arrow: an example of ChR2-YFP-expressing GAC (green). (B) Loose-patch responses of the cell in (A) to a light bar (500 μm × 100 μm) moving at 500 μm/s in eight directions. (C) Voltage-clamp responses (at −70 mV) of the cell in (A) to blue light flashes, showing a fast GAC-activated postsynaptic current (left, arrow), followed by a delayed BC-mediated visual response (left, asterisk). Inset: expanded view of the fast, L-AP4-resistant current. (D) Overlay of the ChR2-current in a GAC (green, at −70 mV) and the fast postsynaptic current in an ON-OFF DSGC (black, −70 mV) in response to a blue light flash. Inset: expanded view, showing an ~2 ms onset delay between the ChR2 current and the postsynaptic response. (E) Dual recording from a pair of GAC and ON-OFF DSGC in the presence of L-AP4, ACET, and HEX, showing voltage-gated currents in GAC in response to depolarizing steps from −70 mV to −45, −35, −25, and −15 mV (top traces, with the Na^+ channel blocker QX 314 in pipette solution) and inward postsynaptic currents in the ON-OFF DSGC at −70 mV (bottom traces). (F and G) Simultaneous recording (at −70 mV) from a pair of ON SAC (F, white arrow) and ON-OFF DSGC (F, yellow arrow), showing delayed, L-AP4-ACET-HEX-sensitive currents in both ON SAC and ON-OFF DSGCa (G, asterisks), and a fast, L-AP4-ACET-HEX-resistant current only in the ON-OFF DSGC, but not the ON SAC (G, arrow). The reduction in the fast response amplitude after drug application, seen in this particular case, was likely due to response rundown after a long recording period but not to pharmacological blockade (see text related to Figure 2). (H and I) An ON DSGC in response to blue light flashes under voltage clamp at −70 mV, showing a fast synaptic response that is resistant to L-AP4 + ACET + HEX. (J) A putative W3 cell (top, shown only in red channel), with narrow, diffuse dendritic ramification in the middle of IPL (bottom, both red and green channels shown). (K) Responses (at −70 mV) of two putative W3 cells from two different retinae to blue light flashes, showing a small peak response and a sustained component. (L) Summary of the peak current response amplitudes (at −70 mV) of different cell types to blue light flashes in the presence of L-AP4 + ACET + HEX. Numbers in parentheses, cells tested. Error bars represent SEM. Drug concentrations: ACET, 10 μM; HEX, 300 μM; and L-AP4, 20 μM. See also Figure S1.

ChR2-expressing GACs in whole-mount retinae of vGluT3-Cre/ChR2-YFP mice with a flash of intense full-field blue light (referred to as "blue light" henceforth), while recording from cells in the ganglion cell layer (GCL) under voltage clamp at the chloride equilibrium potential E_{Cl} (−70 mV). We found that ON-OFF DSGCs, identified based on dendritic morphology and/or response properties to moving light bars (Figures 1A and 1B), responded to blue light activation of GACs with a fast inward current (Figure 1C, arrow), followed, with a delay of 30–50 ms, by a barrage of excitatory synaptic currents (Figure 1C, left, asterisk). The delayed synaptic currents were blocked by the group III metabotropic glutamate receptor agonist L-AP4 (20 μM, which blocks synaptic transmission from PRs to ON BCs [Slaughter and Miller, 1981] [Figure 1C, right]), indicating that they were visually driven inputs from ON bipolar cells (the visually driven response, especially the OFF response, was not present in every cell, due to photo bleaching of PRs by repeated blue light flashes). However, the fast inward current response was resistant to L-AP4 (Figure 1C, right, arrow) and L-AP4 + ACET (10 μM, a KA receptor antagonist [Pinheiro et al., 2013] that blocks synaptic transmission from PRs to OFF BCs in mouse [Borghuis et al., 2014]) + hexamethonium (HEX, 300 μM, a nicotinic blocker) (Figure 1G), suggesting it was evoked by an excitatory neurotransmitter released from GACs. The fast response

was activated within 4–8 ms of the onset of the blue light (Figure 1C, inset), much earlier than the activation of BC-mediated visual responses (40–60 ms after light onset). Compared to the blue light-evoked ChR2 current recorded from GACs in the presence of L-AP4 + ACET (Figure 1D, green trace, peak amplitude at −70 mV: 232 ± 22 pA, n = 13), the onset of the fast synaptic current in the ON-OFF DSGC was delayed by <2 ms (n = 5) (Figure 1D, inset), consistent with a monosynaptic response to an excitatory transmitter released by GACs. Similar responses were found from 57 out of 66 morphologically/physiologically confirmed On-OFF DSGCs.

As previously reported (Grimes et al., 2011), we did not detect any ChR2-YFP expression in BCs or PRs in this mouse line (Figure S1 available online), but some cells in the GCL are ChR2-YFP positive. To exclude the possibility of a blue light-evoked glutamate input from axon collaterals of ChR2-YFP-expressing GCs or from BCs that express a low (microscopically undetectable) level of ChR2-GFP, we made dual patch-clamp recordings from pairs of GACs and ON-OFF DSGCs in the whole-mount retina (Figure 1E; Figure S1) in the presence of L-AP4, ACET, and HEX. Depolarizing a GAC with voltage steps activated Ca^{2+} currents in the GAC (Figure 1E, top traces) and, correspondingly, inward excitatory postsynaptic currents in an overlapping ON-OFF DSGC at −70 mV (Figure 1E, bottom traces). Similar responses were obtained from three successfully recorded pairs of GACs and ON-OFF DSGCs (Figure S1), demonstrating the presence of functional excitatory synapses between individual GACs and ON-OFF DSGCs (see Discussion).

In addition to ON-OFF DSGCs, we also found similar postsynaptic responses to optical activation of GACs from ON DSGCs (Figure 1H). These responses also persisted in the presence of L-AP4 + ACET + HEX (Figure 1I, n = 9), suggesting a direct excitatory input from GACs to ON DSGCs. In contrast, we did not detect any response from SACs (7 ON SACs and 1 OFF SAC) to optical activation of GACs in the presence of L-AP4 + ACET + HEX (Figures 1F and 1G). Because ON SAC dendrites closely cofasciculate with those of ON and ON-OFF DSGCs, this result suggests that GACs make selective excitatory synaptic contacts with specific postsynaptic targets.

We also tested the response of small-soma GCs with dendritic morphologies resembling those of W3 cells (Kim et al., 2010; Zhang et al., 2012) to optical activation of GACs (Figure 1J). Although W3 cells ramify diffusely and overlap with GAC processes in the band between the ON and OFF cholinergic strata in the IPL (Figure 1J) (Kim et al., 2010), we detected only small inward currents (mean peak amplitude at −70 mV: 13.4 ± 8.3 pA, n = 11) in 11 out of 20 putative W3 cells tested in the presence of L-AP4 + ACET + HEX (Figure 1K), with the remaining 9 cells showing no detectable response. We also found that optical activation of GACs evoked fast inward currents in a small number of other types of bistratified and monostratified GCs (including OFF GCs) in the presence of L-AP4 (data not shown), but more extensive studies are required to identify and characterize these cells.

Ca^{2+}-Dependent Excitatory Glutamatergic Transmission from GACs to ON-OFF and ON DSGCs

The blue light-evoked responses in ON-OFF DSGCs (at −70 mV in the presence of L-AP4 and HEX) were largely blocked by the AMPA receptor antagonist GYKI52466 (20 μM, 83.0% ± 4.5% blockade, n = 4), or the AMPA/KA receptor antagonist CNQX (40 μM, 93.9% ± 2.4% blockade, n = 18), but was little affected by the KA receptor-selective antagonist ACET (10 μM, 5.4% ± 1.9% blockade, n = 10) (Figure 2A). L-AP4 or HEX alone did not have a significant effect on the early fast response to blue light (0.4% ± 5.5% blockade, n = 5, or 1.8% ± 13.7% blockade, n = 7, respectively). Application of the muscarinic receptor blocker, atropine (ATRO, 2 μM) also did not have any effect (0.7% ± 4.4% blockade, n = 3). At more depolarized membrane potentials (e.g., −40 mV), a CPP- (20 μM) sensitive NMDA component was also detected (Figure 2B), suggesting that both AMPA and NMDA receptors mediate the glutamatergic synaptic transmission from GACs to ON-OFF DSGCs. The current-voltage (I-V) relation of the peak response showed a J-shaped region, presumably due to voltage-dependent Mg^{2+} block of NMDA currents (Figure 2C, top, black curve); and, in the presence of CNQX (40 μM), a nonlinear NMDA component was clearly resolvable (Figure 2C, top, red curve). In the presence of CPP, L-AP4, HEX, SR95531 (50 μM), and strychnine (1 μM), the I-V relation was nearly linear at negative potentials, but many ON-OFF DSGCs showed a more positive reversal potential than 0 mV ($\sim E_{Cation}$) or an inward rectification at positive membrane potentials (Figure 2C, bottom, Cell 1), possibly due to inadequate voltage clamp at more depolarized potentials. Together, the above results demonstrate functional glutamatergic synaptic transmission from GACs to ON-OFF DSGCs, mediated by postsynaptic AMPA/NMDA receptors.

Because of the relatively low frequency of encountering ON DSGCs in our sample, we only tested a few essential pharmacological agents to confirm the glutamatergic nature of the excitatory transmission from GACs to ON DSGCs. The response of ON DSGCs to optical activation of GACs was resistant to L-AP4 + ACET + HEX (n = 5, Figures 1H and 1I), but completely blocked by CNQX (n = 4) at −70 mV, and partially blocked by CPP (29.8% ± 8.7% blockade of the peak current, n = 3) at −40 mV, indicating fast excitatory glutamatergic synaptic transmission mediated by both non-NMDA and NMDA receptors.

Because ChR2-YFP is also expressed in some cells in the GCL (Figure S1), we only recorded from GCs that did not show any YPF fluorescence. Indeed, ChR2 current was never detected in our recorded GCs because the blue light-evoked response was consistently blocked by glutamate receptor antagonists (Figure 2A). To confirm that blue light-evoked responses in DSGCs were mediated by Ca^{2+}-dependent vesicular transmitter release, but not by direct gap-junction coupling between the recorded DSGCs and ChR2-YFP-expressing cells, we showed that the Ca^{2+} channel blocker, $CdCl_2$ (300 μM), blocked the responses of DSGCs (4 ON-OFF DSGCs, 1 ON DSGC) to blue light stimulation in the presence of L-AP4, ACET, and HEX (Figure 2D). Incubating the retina with the gap junction blocker 18β-GA (25 μM) for 15–45 min also did not block the response of ON-OFF DSGCs to blue light activation of GACs (Figure 2E, n = 6), arguing against a gap junction-mediated current. In contrast, 15 min incubation of 25 μM 18β-GA effectively blocked gap junction-coupled spikelets in superior-preferring ON-OFF DSGCs (n = 4, Figure S2) as previously reported (Trenholm et al., 2013; Xu et al., 2013).

Please cite this article in press as: Lee et al., An Unconventional Glutamatergic Circuit in the Retina Formed by vGluT3 Amacrine Cells, Neuron (2014), http://dx.doi.org/10.1016/j.neuron.2014.10.021

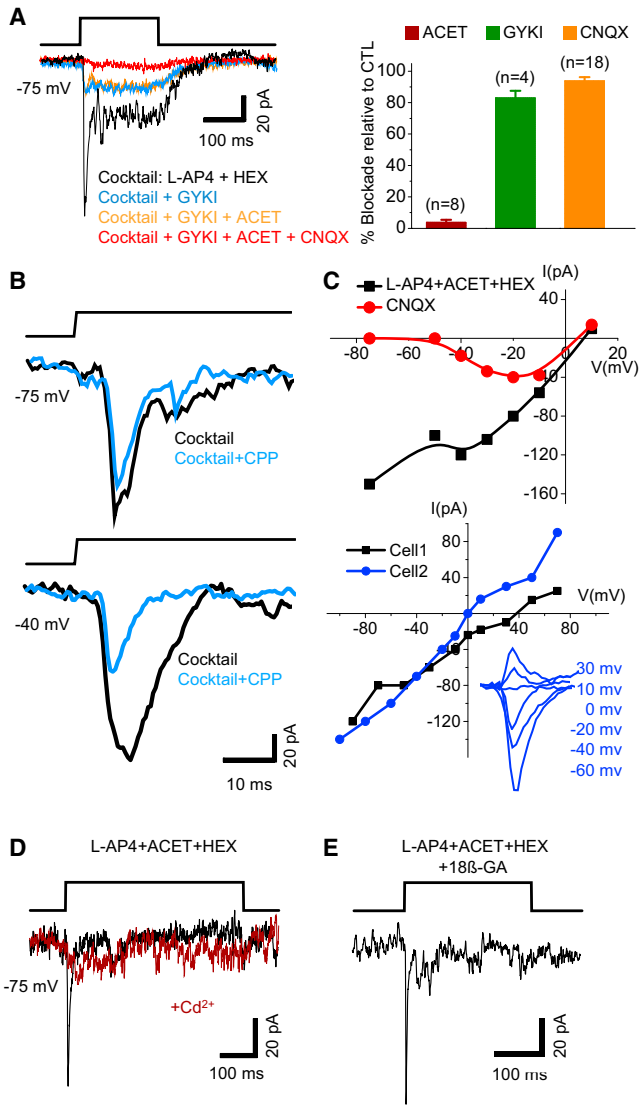

Figure 2. Properties of the Glutamatergic Transmission from GACs to ON-OFF DSGCs

(A) Left, effects of GYKI52466 (GYKI), ACET, and CNQX on the response of an ON-OFF DSGC to blue light flashes recorded at −75 mV in the presence of a control cocktail of L-AP4 and HEX. Right, statistical summary of the effects. Numbers in parentheses, cells tested. Error bars represent SEM (B) Voltage-dependent block of the NMDA component of blue light-evoked responses by CPP in an ON-OFF DSGC. (C) Top: I-V relations of blue light-evoked responses in an ON-OFF DSGC in the presence of L-AP4, ACET, and HEX before (black) and after (red) the addition of CNQX. Bottom: I-V relations of AMPA receptor-mediated responses of two other ON-OFF DSGCs to blue light flashes in the presence of CPP, L-AP4, HEX, ACET, SR95531, and strychnine. (D) $CdCl_2$ blocked the response of an ON-OFF DSGC to blue light stimulation in the presence of L-AP4, ACET, and HEX. (E) A blue light-evoked response in an ON-OFF DSGC remained intact after 25 min incubation in 18β-GA and L-AP4, ACET, and HEX. Drug concentrations : ACET, 10 μM; $CdCl_2$, 300 μM; CNQX, 40 μM; CPP, 20 μM; GYKI, 20 μM; HEX, 300 μM; L-AP4, 20 μM; SR95531, 50 μM; strychnine, 1 μM; 18β-GA, 25 μM. See also Figure S2.

GACs Generate ON-OFF Light Responses, with a Medium-Center, Wide-Surround Receptive Field Structure

Consistent with the dendritic stratification of GACs in both sublamina *a* and *b* (Figure 3A), whole-cell current-clamp recording from GACs in the light-adapted whole-mount retina (see Experimental Procedures) showed a fast depolarization in response to both the onset and offset of a 50-μm-radius light spot at the receptive center (Figure 3B, left, n = 5). However, when stimulated with a large spot (1,000 μm in radius), the same GACs responded with a hyperpolarization, rather than a depolarization, at both light onset and offset (Figure 3B, right, n = 5), suggesting that GACs are strongly inhibited by the receptive field surround. Voltage-clamp recordings further demonstrated that GACs received excitatory and inhibitory synaptic inputs at both light onset and offset (Figure 3C). When the light spot size increased from 50 to 1,000 μm in radius, the excitatory inputs became greatly reduced, while the inhibitory inputs became stronger and more transient (Figure 3C), suggesting a concerted presynaptic feedback suppression of the BC excitatory output and a postsynaptic feedforward inhibition of the GACs by the surround. L-AP4 blocked both the excitatory and inhibitory inputs at the center light spot onset but not at the offset. Subsequent application of ACET on top of L-AP4 eliminated the excitatory and inhibitory inputs at the light offset (Figure 3C), suggesting that GACs received excitatory and inhibitory inputs from both the ON and OFF channels. When stimulated with a light ring of expanding radius (Figure 3D), GACs showed a medium excitatory receptive-field center of ~100 μm in radius and a wide inhibitory surround of up to 1,000 μm in radius (Figure 3E). While the spatial profile (response amplitude versus light annulus radius) of the excitatory input was similar between ON and OFF responses, the spatial profile of the inhibitory input was slightly broader for ON than for OFF responses (Figure 3E), suggesting a relatively stronger wide-field inhibition in the ON input than the OFF.

The inhibitory input from the surround was predominantly mediated by $GABA_A$ receptors because it was blocked completely by SR95531 (50 μM, n = 3, Figures 3F and 3G). However, the inhibitory input at the center could be blocked completely only by a combination of SR95531 (25 μM) and strychnine (1 μM) (Figure 3F, n = 4), suggesting that the center inhibitory input to the GAC was mediated by both glycinergic and GABAergic amacrine cells. When a light bar moved across the receptive field in different directions, GACs gave a depolarizing response to both the leading and the trailing edge of the light bar, but the somatic depolarization showed no detectable directional selectivity (n = 5, Figure S3).

Voltage-clamp recording from GACs (at 0 mV) in the presence of L-AP4 + ACET + HEX showed that blue light evoked outward inhibitory currents in GACs themselves, which could be completely blocked by either SR95531 (50 μM) or CNQX (40 μM) but not by strychnine (2 μM) (Figures 3H and 3I). Since BCs were already inhibited by L-AP4 and ACET, this result suggests that GACs provided an excitatory input to other amacrine cells that, in turn, inhibited GACs via GABAergic synapses. Thus, GACs also make glutamatergic synapses onto certain amacrine cells. Because CNQX blocked all blue light-evoked outward

Please cite this article in press as: Lee et al., An Unconventional Glutamatergic Circuit in the Retina Formed by vGluT3 Amacrine Cells, Neuron (2014), http://dx.doi.org/10.1016/j.neuron.2014.10.021

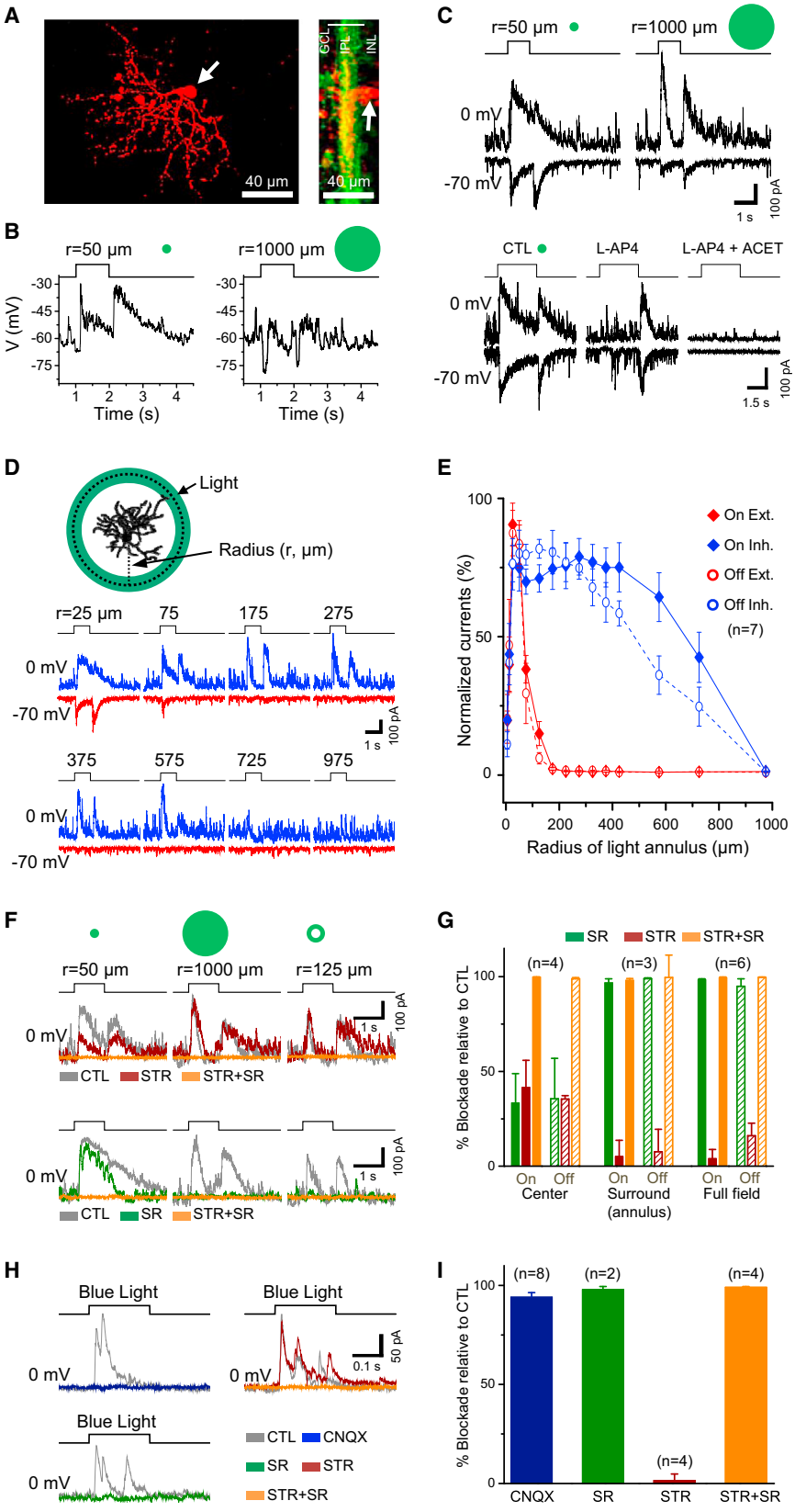

Figure 3. Receptive-Field Properties of GACs

(A) Whole-mount (left) and cross-sectional (right) views of a GAC (red) after whole-cell recording in a vGluT3Cre/ChR2-YFP (green) mouse retina. White arrows, GAC soma. (B) Responses of a GAC to 1-s-long flashes of light spots under current clamp, showing depolarizing ON-OFF responses to a small spot (50 μm in radius, left) and hyperpolarizing ON-OFF responses to a large spot (1,000 μm in radius, right). (C) Top: responses of another GAC under voltage clamp to 1 s light flashes of two different sizes (50 and 1,000 μm in radius, centered on the soma), showing inward ON-OFF EPSC (at −70 mV) and outward ON-OFF IPSC (at 0 mV). Bottom: responses of the same GAC to 3 s flashes of a 50-μm-radius light spot, showing selective blockade of ON responses by L-AP4 and of both ON and OFF responses by L-AP4 and ACET. (D) Responses of a GAC to 1 s flashes of light annuli (50 μm in thickness), showing EPSCs (red, −70 mV) and IPSCs (blue, 0 mV) evoked by light annuli of various radii. (E) Normalized peak EPSCs and IPSCs as a function of annulus radius (n = 7 GACs). Thickness of the annuli was 50 μm, except the smallest two annuli, which were 10 and 25 μm, respectively. (F) Effects of STR and SR (applied in two different sequences) on IPSCs evoked by a center light spot (50 μm in radius, left), a full-field light spot (1,000 μm in radius, center), and a surround light annulus (125 μm in radius, right). (G) Summary of effects of SR and STR on ON-OFF IPSCs evoked by center, surround, and full-field light spot shown in (F). (H) Effects of CNQX, SR, and STR on inhibitory currents (at 0 mV) evoked by blue light stimulation of ChR2-expressing GACs in the presence of L-AP4, ACET, HEX, and atropine. (I) Summary of effects in (H), indicating that blue light evoked glutamate release from GACs onto unidentified amacrine cells, which, in turn, were induced to release GABA onto GACs. Numbers in parentheses, cells tested. Error bars represent SEM. Drug concentrations: ACET, 10 μM; atropine, 2 μM; CNQX, 40 μM; HEX, 300 μM; L-AP4, 20 μM; SR, 50 μM; STR, 2 μM. See also Figure S3.

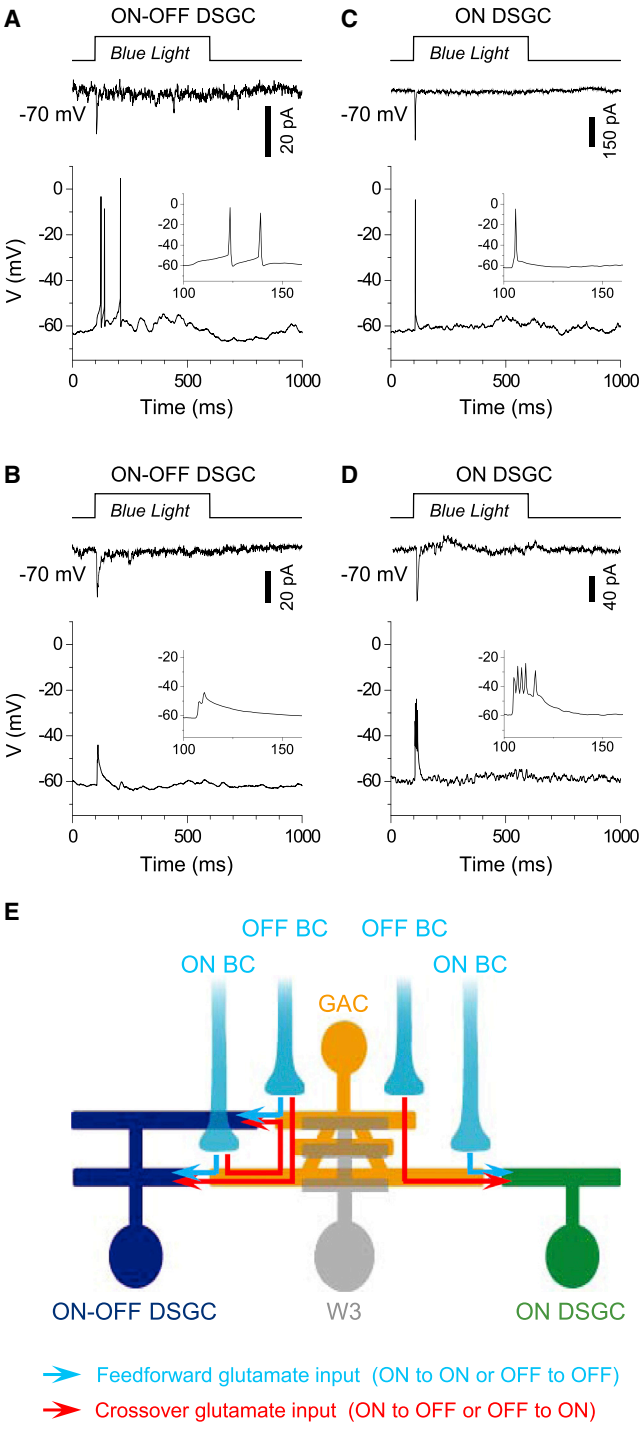

Figure 4. GACs Directly Influence DSGC Spike Patterns

Responses of ON-OFF (A and B) and ON DSGCs (C and D) under voltage (−70 mV, top) and current clamp (0 pA, bottom) to blue light stimulation in the presence of L-AP4, ACET, and HEX, showing examples of transient somatic spikes (A and C) and small (dendritic-like) spikes (B and D). Insets: blown-up view of the voltage responses. (E) Model of the GAC circuit, showing GACs receiving glutamatergic inputs from ON and OFF BCs and sending glutamatergic outputs to ON-OFF and ON DSGCs to mediate feedforward or lateral excitation (blue arrows) and crossover excitations (red arrows). GACs also provide a small excitatory input to a subset of W3 cells (gray). Not shown in the scheme are the strong pre- and postsynaptic inhibition of GACs from the surround and GAC outputs to other unidentified ACs and GCs. See also Figure S4.

current responses of GACs at 0 mV (Figure 3H), this result also suggests that GACs do not make direct inhibitory synapses onto each other even if they should release an inhibitory transmitter (e.g., glycine) in addition to glutamate. Due to the presence of a large ChR2 current in GACs (at −70 mV) during blue light stimulation (Figure 1D), we did not test the possibility that neighboring GACs directly excite each other via glutamatergic synapses.

GACs Directly Influence the Spike Activity of DSGCs

To determine the impact of GACs on DSGC function, we recorded the membrane potential of ON-OFF and ON DSGCs under whole-cell current clamp (with a K^+-based pipette solution, see Experimental Procedures), while activating GACs with blue light. With the light-driven BC output blocked with L-AP4 and ACET (and nicotinic transmission blocked by HEX as a precaution), optical activation of GACs was sufficient to evoke transient spikes from 4 out of the 9 ON-OFF and 2 out of the 3 ON DSGCs tested (Figures 4A and 4C). The remaining 5 ON-OFF DSGCs and 1 ON DSGC gave either a subthreshold depolarization or small spikes (Figures 4B and 4D) that resembled the dendritic spikes previously reported (Oesch et al., 2005). To confirm that the blue light-evoked responses in GACs were within the physiological range, we compared the voltage response of GACs to full-field blue light with that to visual stimulation (center white light spot, without L-AP4 and ACET). The amplitude of the voltage responses was comparable between these two stimulation conditions (n = 7, Figure S4), indicating that GACs provide a physiologically relevant excitatory drive to DSGCs.

Finally, we also investigated whether GACs provide a direct glycinergic drive to ON-OFF DSGCs. In response to blue light in the presence of LAP4 + ACET + CNQX + CPP + HEX, 9 out of the 11 ON-OFF DSGCs tested at 0 mV showed no detectable outward current, suggesting a lack of direct glycinergic or GABAergic synaptic input (Figure S4). The remaining 2 of the 11 cells displayed small (<15 pA), strychnine-sensitive outward currents (Figure S4), but it is unclear whether these small currents were evoked by GACs or potentially by ChR2-expressing ACs in the GCL. Overall, these results indicate a lack of significant (if any) glycinergic synaptic transmission from GACs to DSGCs, consistent with our paired recordings from GACs and ON-OFF DSGCs, which failed to detect any outward current responses from DSGCs at 0 mV (n = 3). However, it remains to be determined whether GACs release glycine onto other cell types.

DISCUSSION

A Noncanonical Glutamatergic Circuit in the Inner Retina

The present study demonstrated functional glutamate release from GACs, contradicting the conventional view that amacrine cells are inhibitory (except SACs, which release both GABA and ACh). We identified ON and ON-OFF DSGCs as

postsynaptic targets of GACs. Because our dual patch-clamp recordings found only small synaptic currents (Figure 1E; Figures S1D and S1E), it seems that each GAC makes only a small number of glutamatergic synapses onto an ON-OFF DSGC and that a DSGC integrates inputs from a number of GACs to generate a sizable whole-cell response. Notably, even though most W3 cell dendrites ramify in the same diffuse band in the IPL as do GAC dendrites (Figure 1J), only a subpopulation (or subtype) of W3 GCs responded to GAC activation, and their responses to full-field blue light activation were much smaller than those of ON-OFF and ON DSGCs (Figure 1K). In addition to DSGCs, a few other bistratified and monostratified (including OFF monostratified) GCs also gave excitatory postsynaptic responses (data not shown) to optical activation of GACs in the presence of L-AP4, though most other GC types recorded were not responsive to GAC activation. As indicated by the data shown in Figure 3H, some ACs may also receive glutamate input from GACs. However, GACs apparently avoid making glutamatergic synapses onto SACs, even though SACs and DSGCs cofasciculate closely. Thus, GACs are expected to influence multiple, but specific, postsynaptic cell types.

The Receptive Field Structure and Potential Functional Role of GACs

We showed that GACs receive excitatory inputs from both ON and OFF BCs and generate ON-OFF depolarization to small center flashes. They also receive strong surround inhibition and generate ON-OFF hyperpolarization to large/full-field flashes. The ON-OFF center response implies that GACs can integrate excitatory inputs from separate ON and OFF channels into an ON-OFF glutamatergic output at individual output synapses. This glutamatergic synaptic organization contrasts the current dogma that ON and OFF channels are segregated in the IPL, and that ON and OFF channels typically inhibit each other through diffuse, narrow-field glycinergic amacrine cells (crossover inhibition) (Werblin, 2010), but do not excite each other through excitatory synapses. We propose that GACs provide a mechanism for "crossover excitation," in which ON channel excites the OFF channel and vice versa (Figure 4E, red arrows). This circuit can potentially enhance the ON-OFF response of bistratified or diffusely stratified cells, such as ON-OFF DSGCs, by coordinating/synergizing the responses between the ON and OFF dendrites, thus providing an additional level of processing between ON and OFF channels. There is currently no evidence that GACs interfere with directional computation of ON-OFF DSGCs, since the glutamatergic input from GACs is relatively small compared to the input from BCs and is likely counterbalanced by a strong asymmetric GABAergic input from SACs during null direction movement, in analogy to the situation in which the cholinergic input to a DSGC is rendered ineffective during null direction movement (Lee et al., 2010). The somatic responses of GACs suggest that these cells are not direction selective, though we cannot rule out the possibility of directional glutamate release at GAC dendrites or directional connectivity with DSGC dendrites.

Notably, even some monostratified cells, such as ON DSGCs, also receive presumably ON-OFF glutamate signals from GACs. Although most monostratified GCs are so far not known to generate ON-OFF center responses, ON DSGCs (including those that do not have ectopic OFF dendritic branches) in the mouse retina have been reported to receive L-AP4-resistant OFF excitation (Ackert et al., 2009; Farajian et al., 2011; S. He et al., 2005, Invest. Ophthalmol. Vis. Sci., abstract; Sun et al., 2006). The functional role of this OFF excitatory input is currently unclear, but it is known that the OFF center responses in ON GCs (and vice versa) are often masked by GABAergic inhibition (Farajian et al., 2011), which may be attributable, in part, to the receptive field properties of GACs (Figure 3). It has been recently reported that many OFF GCs give ON responses under certain adaptation conditions (T.A. Munch and A. Tikidji-Hamburyan, 2014, Invest. Ophthalmol. Vis. Sci., abstract). These anomalous responses, while difficult to explain by the canonical glutamatergic circuits, seem compatible with the GAC circuit. Finally, GACs may also play a role in lateral excitation, especially in predicting local lateral movement (Berry et al., 1999) and in synchronizing responses among GCs over a medium spatial range (Brivanlou et al., 1998; Mastronarde, 1983; Meister et al., 1995; Schnitzer and Meister, 2003).

EXPERIMENTAL PROCEDURES

vGluT3-Cre/ChR2-YFP mice (4–10 weeks old) were generated by crossbreeding vGlut3-Cre mice (Grimes et al., 2011) with ChR2-YFP mice (strain B6;129S-*Gt(ROSA)26Sor*$^{tm32(CAG-COP4*H134R/EYFP)Hze}$/J, Jackson Laboratory). All animal procedures were approved by Yale University IACUC. Patch-clamp recordings were made in the whole-mount retina in oxygenated ACSF (125 mM NaCl, 2.5 mM KCl, 2 mM $CaCl_2$, 1 mM $MgCl_2$, 1.25 mM NaH_2PO_4, 0.5 mM L-glutamine, 26 mM $NaHCO_3$, and 20 mM glucose [pH7.4]) at 32°C–34°C. Pipette solution contained for loose patch: ACSF; for voltage clamp: 105 mM $CsMeSO_4$, 0.5 mM $CaCl_2$, 10 mM HEPES, 5 mM EGTA, 5 mM Na_2-phosphocreatine, 2 mM ATP-Mg, 0.5 mM GTP-2Na, 2 mM ascorbic acid, 8 mM QX314-Cl [pH 7.2] with 20–30 CsOH; and for current clamp: 105 mM potassium gluconate, 5 mM KCl, 0.5 mM $CaCl_2$, 2 mM $MgCl_2$, 5 mM EGTA, 10 mM HEPES, 5 mM Na_2-phosphocreatine, 2 mM ATP-2Na, 0.5 mM GTP-2Na, 2 mM ascorbic acid [pH 7.2], with 5 mM NaOH and 15 mM KOH. Recorded cells were filled with Alexa Fluor 594 and imaged under a two-photon microscope, ChR2 was activated by full-field flashes of blue light (λ_{peak}, 460–470 nm; intensity at retina: 2–5.5 × 10^{10} photons μm^{-2} s^{-1}). GACs were identified under brief (2–10 s each time, 2–5 times in total) epifluorescence illumination (10^{10} photons $\mu m^{-2}s^{-1}$ at retina, 465 ± 15 nm in wavelength) and recorded under white light (transillumination, 10^5 photons $\mu m^{-2}s^{-1}$ at retina). Stable light responses were obtained from GACs after 1–5 min of dark adaptation following the establishment of a patch-clamp configuration. Visual stimulus patterns were generated on a black-and-white LCD (contrast: 100:1; maximum image intensity at retina: ~2 × 10^5 photons $\mu m^{-2}s^{-1}$) and projected to the retina via the microscope condenser lens. Drugs were applied at the same concentrations as first described in the text. Results were expressed as mean ± SEM. Statistical significance was determined at the level of α = 0.05 by paired Student's t test (Figure S4B). See additional information in Supplemental Experimental Procedures.

SUPPLEMENTAL INFORMATION

Supplemental Information includes Supplemental Experimental Procedures and four figures and can be found with this article online at http://dx.doi.org/10.1016/j.neuron.2014.10.021.

AUTHOR CONTRIBUTIONS

S.L. recorded from GACs and GAC-DSGC pairs and characterized the responses in DSGCs and other cells; L.C. discovered GAC input to DSGCs and characterized the responses in DSGCs and other cells; M.C.

characterized the responses in DSGCs and other cells; M.Y. participated in initial optogenetic experiments; R.P.S. generated the vGluT3Cre mouse and did immunochemical analysis; Z.J.Z. designed the study, analyzed results, and wrote the paper. All authors contributed to the discussion and completion of the paper.

ACKNOWLEDGMENTS

This work was supported by grants from NIH R01EY17353 (Z.J.Z.), NIH T32 EY22312 (Z.J.Z. and M.Y.), and Research to Prevent Blindness (R.P.B.) Unrestricted Grant to Yale Eye Center, and by the Marvin L. Sears Endowed Professorship (Z.J.Z.). We thank Dr. Shigang He for scientific discussions.

Accepted: September 29, 2014
Published: November 6, 2014

REFERENCES

Ackert, J.M., Farajian, R., Völgyi, B., and Bloomfield, S.A. (2009). GABA blockade unmasks an OFF response in ON direction selective ganglion cells in the mammalian retina. J. Physiol. *587*, 4481–4495.

Berry, M.J., 2nd, Brivanlou, I.H., Jordan, T.A., and Meister, M. (1999). Anticipation of moving stimuli by the retina. Nature *398*, 334–338.

Borghuis, B.G., Looger, L.L., Tomita, S., and Demb, J.B. (2014). Kainate receptors mediate signaling in both transient and sustained OFF bipolar cell pathways in mouse retina. J. Neurosci. *34*, 6128–6139.

Brivanlou, I.H., Warland, D.K., and Meister, M. (1998). Mechanisms of concerted firing among retinal ganglion cells. Neuron *20*, 527–539.

El Mestikawy, S., Wallén-Mackenzie, A., Fortin, G.M., Descarries, L., and Trudeau, L.E. (2011). From glutamate co-release to vesicular synergy: vesicular glutamate transporters. Nat. Rev. Neurosci. *12*, 204–216.

Farajian, R., Pan, F., Akopian, A., Völgyi, B., and Bloomfield, S.A. (2011). Masked excitatory crosstalk between the ON and OFF visual pathways in the mammalian retina. J. Physiol. *589*, 4473–4489.

Fremeau, R.T., Jr., Burman, J., Qureshi, T., Tran, C.H., Proctor, J., Johnson, J., Zhang, H., Sulzer, D., Copenhagen, D.R., Storm-Mathisen, J., et al. (2002). The identification of vesicular glutamate transporter 3 suggests novel modes of signaling by glutamate. Proc. Natl. Acad. Sci. USA *99*, 14488–14493.

Gong, J., Jellali, A., Mutterer, J., Sahel, J.A., Rendon, A., and Picaud, S. (2006). Distribution of vesicular glutamate transporters in rat and human retina. Brain Res. *1082*, 73–85.

Grimes, W.N., Seal, R.P., Oesch, N., Edwards, R.H., and Diamond, J.S. (2011). Genetic targeting and physiological features of VGLUT3+ amacrine cells. Vis. Neurosci. *28*, 381–392.

Haverkamp, S., and Wässle, H. (2004). Characterization of an amacrine cell type of the mammalian retina immunoreactive for vesicular glutamate transporter 3. J. Comp. Neurol. *468*, 251–263.

Johnson, J., Sherry, D.M., Liu, X., Fremeau, R.T., Jr., Seal, R.P., Edwards, R.H., and Copenhagen, D.R. (2004). Vesicular glutamate transporter 3 expression identifies glutamatergic amacrine cells in the rodent retina. J. Comp. Neurol. *477*, 386–398.

Kim, I.J., Zhang, Y., Meister, M., and Sanes, J.R. (2010). Laminar restriction of retinal ganglion cell dendrites and axons: subtype-specific developmental patterns revealed with transgenic markers. J. Neurosci. *30*, 1452–1462.

Lee, S., Kim, K., and Zhou, Z.J. (2010). Role of ACh-GABA cotransmission in detecting image motion and motion direction. Neuron *68*, 1159–1172.

Masland, R.H. (2012). The neuronal organization of the retina. Neuron *76*, 266–280.

Mastronarde, D.N. (1983). Correlated firing of cat retinal ganglion cells. I. Spontaneously active inputs to X- and Y-cells. J. Neurophysiol. *49*, 303–324.

Meister, M., Lagnado, L., and Baylor, D.A. (1995). Concerted signaling by retinal ganglion cells. Science *270*, 1207–1210.

Oesch, N., Euler, T., and Taylor, W.R. (2005). Direction-selective dendritic action potentials in rabbit retina. Neuron *47*, 739–750.

Pinheiro, P.S., Lanore, F., Veran, J., Artinian, J., Blanchet, C., Crépel, V., Perrais, D., and Mulle, C. (2013). Selective block of postsynaptic kainate receptors reveals their function at hippocampal mossy fiber synapses. Cereb. Cortex *23*, 323–331.

Schnitzer, M.J., and Meister, M. (2003). Multineuronal firing patterns in the signal from eye to brain. Neuron *37*, 499–511.

Slaughter, M.M., and Miller, R.F. (1981). 2-amino-4-phosphonobutyric acid: a new pharmacological tool for retina research. Science *211*, 182–185.

Stella, S.L., Jr., Li, S., Sabatini, A., Vila, A., and Brecha, N.C. (2008). Comparison of the ontogeny of the vesicular glutamate transporter 3 (VGLUT3) with VGLUT1 and VGLUT2 in the rat retina. Brain Res. *1215*, 20–29.

Sun, W., Deng, Q., Levick, W.R., and He, S. (2006). ON direction-selective ganglion cells in the mouse retina. J. Physiol. *576*, 197–202.

Trenholm, S., McLaughlin, A.J., Schwab, D.J., and Awatramani, G.B. (2013). Dynamic tuning of electrical and chemical synaptic transmission in a network of motion coding retinal neurons. J. Neurosci. *33*, 14927–14938.

Wässle, H., Puller, C., Müller, F., and Haverkamp, S. (2009). Cone contacts, mosaics, and territories of bipolar cells in the mouse retina. J. Neurosci. *29*, 106–117.

Werblin, F.S. (2010). Six different roles for crossover inhibition in the retina: correcting the nonlinearities of synaptic transmission. Vis. Neurosci. *27*, 1–8.

Xu, Z., Zeng, Q., Shi, X., and He, S. (2013). Changing coupling pattern of The ON-OFF direction-selective ganglion cells in early postnatal mouse retina. Neuroscience *250*, 798–808.

Zhang, Y., Kim, I.J., Sanes, J.R., and Meister, M. (2012). The most numerous ganglion cell type of the mouse retina is a selective feature detector. Proc. Natl. Acad. Sci. USA *109*, E2391–E2398.

Neuron, Volume *84*

Supplemental Information

An Unconventional Glutamatergic Circuit in the Retina Formed by vGluT3 Amacrine Cells

Seunghoon Lee, Lujing Chen, Minggang Chen, Meijun Ye, Rebecca P. Seal, and Z. Jimmy Zhou

Supplemental Information

Inventory of Supplemental Information

1. Figure S1 and legend, related to Figure 1.
2. Figure S2 and legend, related to Figure 2.
3. Figure S3 and legend, related to Figure 3.
4. Figure S4 and legend, related to Figure 4.
5. Supplemental Experimental Procedures.

Supplemental Figures and Legends

Figure S1

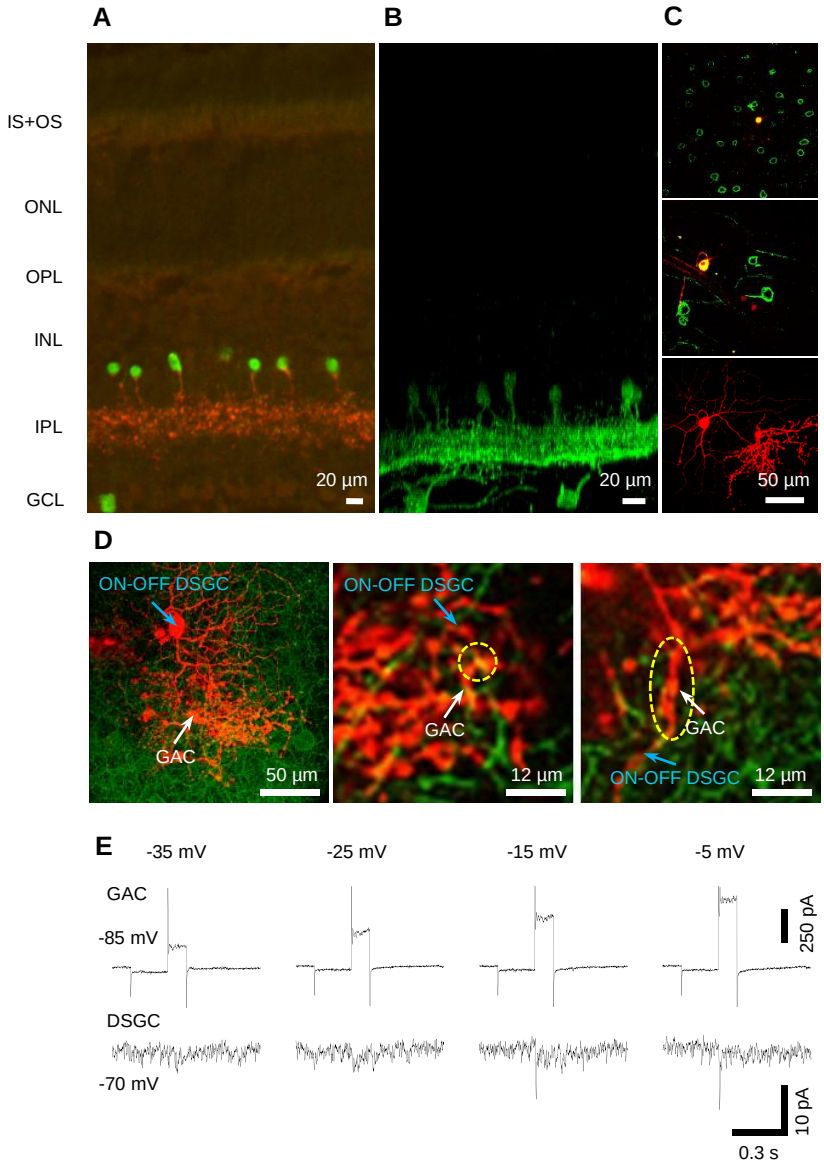

Figure S1 (related to Figure 1). (A-C) Anti-vGluT3 antibody and ChR2-YFP labeling of GACs. (A) Thin (25 µm) retinal section from a vGluT3-Cre/Rosa26YFP mouse, showing YFP expression (green) in GACs in the INL and a small number of neurons in the GCL. YFP-positive GACs are exclusively immunoreactive to a guinea pig anti-vGluT3 antibody (from R. Edwards, University of California at San Francisco, at

1:5000 dilution). (B) z-Projection of a two-photon image stack taken from a wholemount vGluT3-Cre/ChR2-YFP mouse retina, showing ChR2-YFP expression in a regular population of GACs in the IPL and an irregular, heterogeneous population of neurons in the GCL. No YFP expression was detected in other neurons in INL, OPL, ONL, IS, or OS (A, B), except occasionally in Müller cells (not shown). (C) Two-photon images of the same retina as in (B), showing ChR2-YFP-expression in a regular, homogeneous population of GACs in INL (top) and irregular, inhomogeneous populations of neurons in GCL (middle). A pair of ChR2-YFP-expressing GAC (yellow, top panel) and putative ON DSGC (yellow, middle panel) were filled with Alexa 594 during dual whole-cell patch recording, revealing their dendritic morphology in a collapsed image from maximal-intensity projection of a two-photon image stack (bottom). No glutamatergic transmission was detected in this pair, presumably due to a lack of dendritic overlap. **(D-E) Glutamatergic transmission between GAC and ON-OFF DSGC under dual patch clamp.** (D) Left: whole-mount view of a maximally projected image of a pair of GAC and ON-OFF DSGC filled with Alexa 594 (red) during dual whole-cell recording in vGluT3-Cre/ChR2-YFP (green) retina, showing dendritic overlap between the two cells. Arrows: ON-OFF DSGC (blue) and ChR2-expressing GAC (white). Center and Right: whole-mount view of single two-photon optical sections, showing examples of dendritic crossing between the GAC (white arrow) and ON-OFF DSGC (blue arrow) in the ON sublamina (Center), and dendritic co-fasciculation in the OFF sublamina (Right). (E) Dual whole-cell recording from the same pair in (D) in the presence of L-AP4 (10 µM), ACET (10 µM), and HEX (300 µM), showing (in upper traces) voltage-gated currents in the GAC in response to depolarizing steps to -35, -25, -15, and -5 mV (100 ms in

duration, preceded by a 200-ms pre-step from -85 to -100 mV) and (in lower traces) inward postsynaptic currents in the ON-OFF DSGC at -70 mV. The presynaptic threshold for activating a detectable postsynaptic response (between -35 and -25 mV, n=3 pairs) is consistent with the activation voltage range of Ca^{2+} channels in GACs previously reported (Grimes et al., 2011), but this measured threshold voltage could have been affected by potential inadequacy in voltage clamp and/or presynaptic Ca^{2+} channel rundown under whole cell recording. No outward postsynaptic current (at holding potential 0 mV) was detected in these recordings.

Figure S2

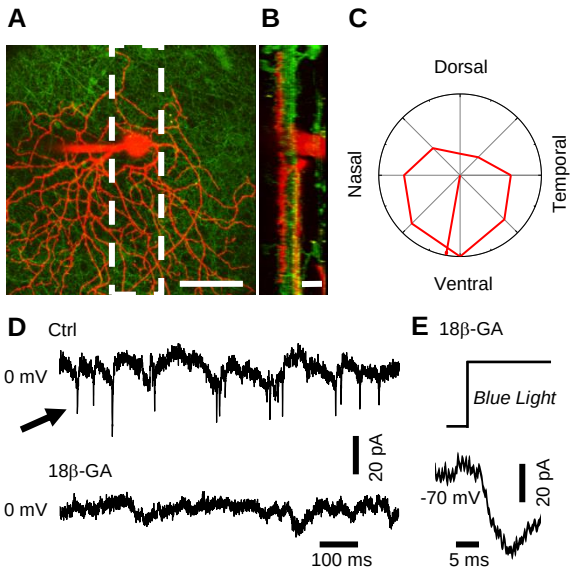

Figure S2 (related to Figure 2). Pharmacological effects of 18β-GA on gap junction-coupled spikelets in ventrally preferred ON-OFF DSGC. (A) Collapsed two-photon image (maximal projection from a z-stack) of an ON-OFF DSGC (filled with a red dye during patch clamp) in a vGluT3-Cre/ChR2-YFP (green) retina, showing a ventrally pointing, asymmetric dendritic field. Scale bar: 50 µm. (B) z-Projection of the

same image stack as in (A, boxed area selected). Scale bar: 20 µm. (C) Directional tuning curve from loose-patch recording of the cell in (A) in response to a white light bar (500x100 µm) moving (500 µm/s) in eight different directions, showing a ventrally preferred direction (superior coding visual field). (D) Gap junction-coupled spikelets (arrow, top trace) in the same ON-OFF DSGC shown in (A), evoked by voltage-clamping the same cell to 0 mV, which activated spikes in neighboring coupled superior coding ON-OFF DSGCs (Trenholm et al., 2013). Bath application of 18β-GA (25 µM, for 13 min) blocked the spikelets, indicating the effectiveness of the drug in blocking gap junction coupling between ON-OFF DSGCs (lower trace). (E) Blue light-evoked response remained intact after 14 minutes of 18β-GA (25 µM) application in the same ON-OFF DSGC.

Figure S3

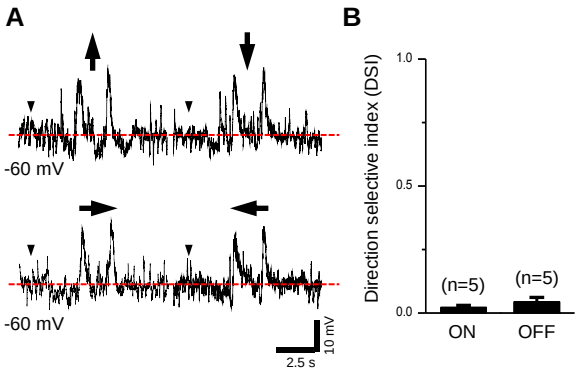

Figure S3 (related to Figure 3). Somatic voltage responses of GACs to a moving light bar. (A) Example traces of current-clamp recording from a GAC in response to a white light bar (600x200 µm) moving (300 µm/s) in four orthogonal directions (arrows), showing ON and OFF depolarizing responses to the leading and the trailing edge of the

moving bar. A small hyperpolarization is discernable preceding the depolarization, presumably due to surround inhibition. No obvious directional preference was detected in somatic voltage responses. Broken red line: resting membrane potential (-60 mV); triangle: onset of moving white bar stimulation, with the leading edge emerging 900 µm away from soma of GAC. (B) Summary of direction selective index (DSI, defined below) from five GACs, showing no direction selectivity.

$$\mathrm{DSI} = \frac{\sqrt{(\mathrm{R}_0 - \mathrm{R}_{180})^2 + (\mathrm{R}_{90} - \mathrm{R}_{270})^2}}{\mathrm{R}_0 + \mathrm{R}_{90} + \mathrm{R}_{180} + \mathrm{R}_{270}}$$

where R_0, R_{90}, R_{180}, and R_{270} are amplitudes of peak depolarization to a light bar moving in the four orthogonal directions, respectively. Error bars: SEM.

Figure S4

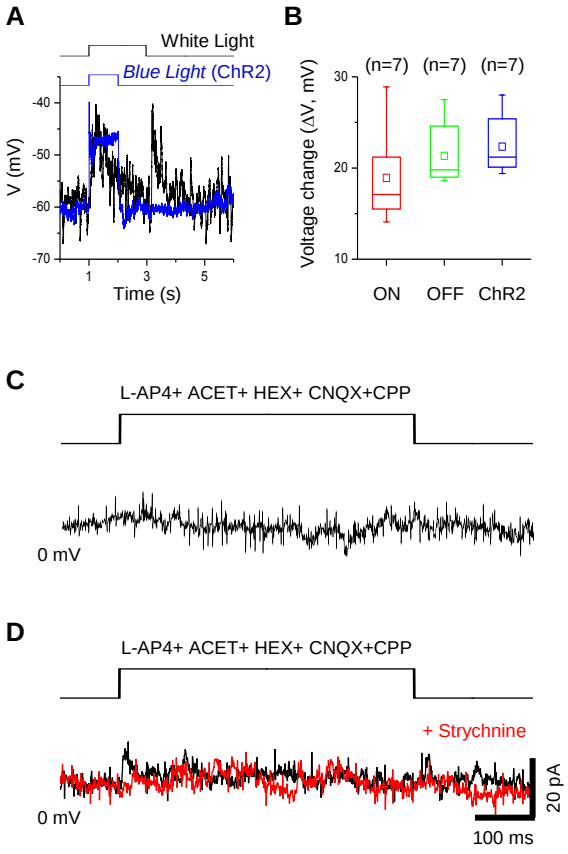

Figure S4 (related to Figure 4). (A, B) Comparison of somatic voltage responses of GACs to visual input and blue light activation of ChR2. (A) Voltage responses of a ChR2-expressing GAC to 2s-long flashes of a center light spot (black trace, 60 µm in radius) and to 1s-long blue light stimulation of ChR2 (blue trace). ChR2 stimulation was conducted in the presence of light-response blocking antagonist cocktail, L-AP4 (20 µM), ACET (20 µM) and HEX (300 µM). (B) Statistical summary of the range (ΔV) of membrane depolarization from resting membrane potentials, showing overlaps in response amplitudes to center light spot and ChR2 stimulations. Resting membrane potentials were not significantly changed after application of the light-response blocking cocktail (slightly hyperpolarized from -58.9 ± 1.9 to -59.7 ± 3.3 mV; mean ± S.D., p=0.67, paired Student's *t*-test). (Bottom and top of the box: 1st and 3rd quartile, respectively; horizontal line in the box: median (2nd quartile); square in the box: mean; whiskers at bottom and top: min and max, respectively). **(C, D) Little or no glycinergic synaptic transmission detected from ON-OFF DSGCs to GACs.** (C) An example of voltage-clamp recording (at 0 mV) from an ON-OFF DSGC, showing no detectable outward postsynaptic current in response to blue light stimulation in the presence of L-AP4 (20 µM), ACET (10 µM), HEX (300 µM), CNQX (40 µM) and CPP (20 µM). Similar results were obtained in 9 out of 11 ON-OFF DSGCs tested. (D) Responses of an ON-OFF DSGC to blue light stimulation (black trace) at 0 mV in the presence of L-AP4 (20 µM), ACET (10 µM), HEX (300 µM), CNQX (40 µM) and CPP (20 µM), showing small (~10 pA) outward postsynaptic currents. This small current was blocked by strychnine (1 µM). Only 2 out of 11 ON-OFF DSGCs tested showed small strychnine-sensitive outward currents similar to shown here.

Supplemental Experimental Procedures

Patch-clamp recording, visual stimulation, two-photon imaging and optical activation of ChR2 in the whole-mount mouse retina

Mouse retinas were dissected under dim red or dim white light illumination. Patch-clamp recordings were made from GCs and SACs in the whole-mount retina under visual control with IR-DIC optics of an Olympus BX51WI upright microscope (with a 60×, 1.0 NA objective, LUMPlanFL/IR, Olympus USA, New York) and an IR video camera (Hamamatsu, Model C2400, Artian Technology Group, Champaign, IL). GACs were identified under brief epi-fluorescence illumination and recorded under dim trans-illumination from the same microscope (Olympus BX51WI). Stable light responses were obtained from GACs after 1-5 min of dark adaptation following the establishment of a patch clamp configuration. Electrophysiological data were recorded with a Multiclamp 700B patch-clamp amplifier (Molecular Devices, CA), stored on Power Lab (AD Instruments, Colorado Springs, CO), and analyzed with pClamp10 (Molecular Devices) and Origin 9 software (Origin Lab Corp., Northampton, MA). Liquid junction potential was calculated using pClamp 10 software and corrected. Pharmacological agents were applied to the retina *via* bath perfusion.

Visual stimuli were generated with the software VisionWorks (Vision Research Graphics, Inc, Durham, NH) on a miniature black-and-white transmissive LCD (diagonal dimension: 18 mm; resolution: 800 × 600 pixel; refresh rate: 60 Hz; contrast ratio: 100:1; Model: SGA4LCD, CRL Opto Ltd., Dunfirmline, Scotland), which was illuminated by a 100-W halogen bulb from the microscope trans-illumination port. The stimulus image on the LCD screen was projected through the microscope condenser lens onto

photoreceptor outer segments of the retina. The visual stimulus intensity at the retina was 0.006 nW μm^{-2} (~2×10^5 photons μm^{-2} s^{-1}) with an intensity-weighted mean wavelength of 573 nm.

Z-series stacks of two-photon images of ChR2-YFP-expressing cells and whole-cell patch-clamped cells (filled with Alexa Fluor 594) in the whole-mount retina were taken with a two-photon imaging system (Ultima, Prairie Technologies, Middleton, WI), which was configured on the same Olympus BX51WI microscope with a Ti:Sapphire pulsed laser (MaiTai, Newport, CA) tuned to 910-920 nm. Images were processed with Prairie View (Prairie Technologies) and Image J (http://rsb.info.nih.gov/ij).

ChR2 was activated by intense blue light from either a high power LED (λ_{peak}, 470 nm) focused on the retina through the condenser lens of an Olympus BX51WI upright microscope, or from an epi-fluorescence light source (100W Hg bulb, band-pass filtered at 465 ± 15 nm, focused on the retina through the 60×, NA/0.9 objective lens, and controlled by a Uniblitz shutter, Vincent Associates, Rochester, New York). The intensity of the blue light measured at the retina was 22 nW μm^{-2} (5.5 $x10^{10}$ photons μm^{-2} s^{-1}) and 8 nW μm^{-2} ($2x10^{10}$ photons μm^{-2} s^{-1}) for the blue LED and the Hg bulb, respectively.

Histology

Immunostaining of retinal sections was done as described (Grimes et al., 2011). Eyes were postfixed for 2 h and then rinsed in 0.1 mM phosphate buffer (PB). Cornea was cut away, lens removed, and eyecup cryoprotected overnight in 30% sucrose. Sections (16 µm thick) were cut in eyecups on a cryostat and were blocked in PBS plus 5% normal

donkey serum and 0.25% Triton X-100. The sections were then incubated with a guinea pig anti-VGLUT3 antibody at 1:5000 (R. Edwards Lab) in blocking buffer for 1–3 days at 4°C. Sections were washed in the same buffer and then incubated with secondary antibodies at room temperature for 2 h.